IMPROVING ACCURACY IN ROBOTIZED FIBER PLACEMENT

Maylis Uhart, Olivier Patrouix, Yannick Aoustin, Joseph Canou

IMPROVING ACCURACY IN ROBOTIZED FIBER PLACEMENT

M. Uhart[1,2]*, O. Patrouix[1], Y. Aoustin[2], J. Canou[1]
[1] ESTIA, ESTIA Recherche, Technopole Izarbel, 64210 Bidart, France
[2] L'UNAM, Institut de Recherche en Communications et Cybernétique de Nantes UMR CNRS 6597, CNRS, Université de Nantes, 1 rue de la Noë, 44321 Nantes Cedex 3, France
* Corresponding author (m.uhart@estia.fr)

Keywords: *Advanced Fiber Placement, Robotics, Accuracy, Position/Force hybrid control*

Abstract: Material composites are increasingly used in the demanding field of aeronautics. To meet this growing need, *Coriolis Composites* has developed a solution of automated fiber placement named AFP. This system uses a manipulator arm composed of six axes. This fiber placement task requires a compacting strength adapted to the material used. The robot must keep in contact with the mold and control the compacting force. A manipulator arm is not made to work in force, so accuracy problems appear. Within this framework, the industrial project IMPALA was born in order to improve this new process. This paper shows the use of hybrid position-force control to handle the compacting strength in first time and to improve the fiber placement accuracy.

1 General Introduction

Nowadays, many industries (planes, automotive, marine, sport, wind energy) use, or think to use, composite material for manufacturing their mechanical structures.

Because of strong rules for emissions regulation, the industrials have to reduce weight of their products and the petrol consumption. The use of composite materials is advantageous thanks to their specific mechanical characteristics that offer weight reduction compared to metal structures. Also composite allows an optimal layout of the material.

Among the advantages of composite one can also list design flexibility and ease of shaping, levity, resistance, good behavior in time as well as the absence of corrosion [1]. These advantages will also allow increasing cost competitiveness of manufactured products like wind energy machines compared to other energy sources.

For these reasons, the use of composite material will take a significant part in manufacturing processes in industries during the next year (Fig.1) [2] [3].

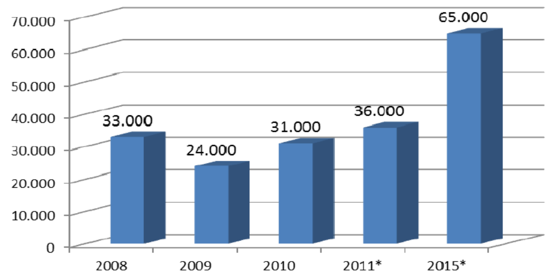

Fig.1. Global European demand (unit in ton) for carbon fibers 2008-2015 [3]

However industry like car industry, doing mass production, uses robots to perform many tasks, and for a wide spreading of composite there is a need to robotize many of composite assembling tasks.

Indeed, today the most part of composite assembling is made manually. Despites the high level of skills of composite worker, there is a lack of repeatability on large and complex structures as well as a lowering of productivity and rapidity compare to what could be the "same but robotized" process [4].

Also the dexterity and repeatability of a robot allows the deposit of fibers and not only tapes, allowing the placement on a more precise or complex shape.

Consequently, research work has been carried on the fiber placement process to use robots [5] in order to have better repeatability and accessibility.

Indeed, the innovation is needed to bring improvement in production efficiency and cost (automation will also contribute to reduce composites production cost).

The company *Coriolis Composites*, has developed a solution for robotic fiber placement that will be presented in this paper. Since 2001, the company filed 12 international patents not only on the AFP systems (Automated Fiber Placement) but also on the equipments and the algorithms. This company made the engineering of the laying head and the software using most of industrial components. The robotic cell (Fig.2) is made of a KUKA KRC240 (6 axes), a 16 meters rail (1 axis) allowing the robot to move, a positioning system (1 axis) allowing to change the orientation of workpiece and draping surface on a vacuum table. Thus, 8 axes have to be synchronized. The 16 carbon fiber coils are located in a creel, and they are guided to the placement tool using the umbilical fibers guide. So the head can lay-up a tape of 101.6 mm composed of 16 carbon fibers of 6.35 mm (¼”). According to the material and heating temperatures to be achieved, an infrared lamp or a diode laser is used to heat the wrapping area.

One of the project’s aims is to improve the accuracy of robotized fiber placement. To do that, there are four objectives. Firstly, we identify the source of errors and understand the mechatronic system. Then, we find the control strategy most relevant and adjust the accuracy control of the laying-up. The AFP systems use very large compacting strength. So, we decide to put on the robot a force sensor to make fiber placement driving the force of the head on the mold. This is a new industrial approach that has not been previously studied.

This paper describes the task of fiber placement in section 2 and its modeling in section 3. Section 4 describes the sensor-based control implemented in section 5. Conclusion and future works are presented in section 6.

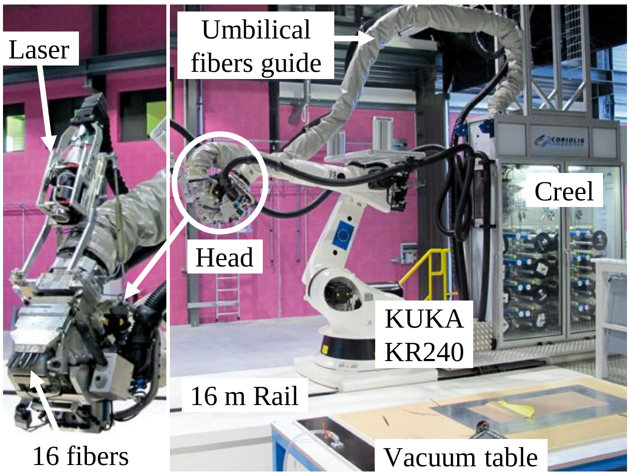

Fig.2. Robotic cell for Fiber Placement

2 Industrial context

2.1 Description of the current system

Coriolis Composites has developed two software programs, named CATFiber and CADFiber, to allow the laying-up. Software needs the CAD data of workpiece to create carbon plies according to the different orientations. Then, software can generate tapes definition in the chosen direction. Finally, the tool-path of the laying head is generated. It is a succession of linear movements (Fig.3).

The process uses a compacting strength more or less important according to the material used which can go up to 1500 N. In the laying head, there is a pneumatic cylinder upstream of the compacting roller to apply the compacting strength on the material. This force must be normal to the surface. So the head orientation is constrained. The description of the compacting strength is in Fig.4. When the tool is put in place, the pneumatic cylinder is controlled in position to produce the force. From a force point of view this is an open loop control; there no direct link between the air pressure and applied force (on the roller) controls.

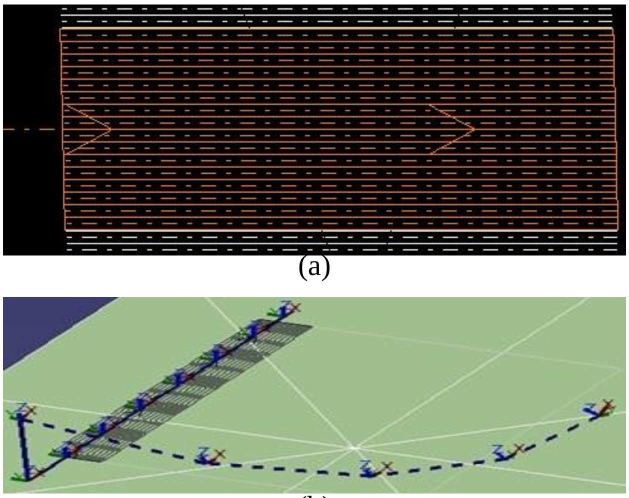

(a)

(b)

Fig.3. Process (a) Tapes (b) Tool trajectory

2.2 Observations

Within this implementation, some inaccurate fibers placements occur, resulting an inadequate quality of workpiece in some sectors such as aeronautics. The defects can be a gap or an overlap between two tapes because of a different fibers placement between theoretical tool-path and real tool-path. Moreover, for certain industrial, overlap is forbidden. This can lead to limited speed of the layup and complex management of the heating unit.

3 Proposal

3.1 Task modeling

The fiber placement task needs a dual command between force and position but also between torque and orientation. In first approach, the compacting roller is considered as not deformable and the rolling without slipping. Consequently, each direction of the tool has to be controlled only in force or in position. This dual command is described in Fig.4. The x-axis direction must be controlled in position $\mathbf{P_x}$ (tool-path) and in torque $\mathbf{T_x}$ (distribution of the force). The y-axis direction must be controlled in position $\mathbf{P_y}$ (tool-path) and in orientation $\mathbf{O_y}$ (head normal to the surface). The z-axis direction must be controlled in force $\mathbf{F_z}$ (compacting strength) and in orientation $\mathbf{O_z}$ (tool-path).

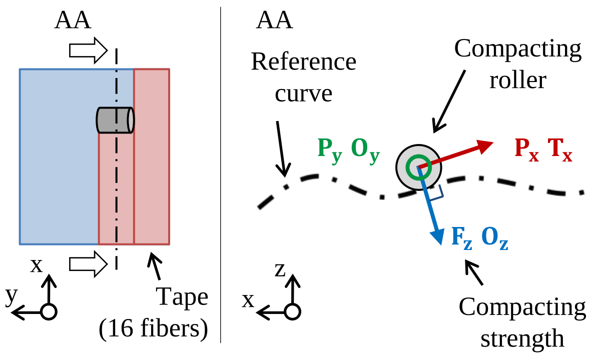

Fig.4. Dual command: force $\mathbf{F_{i\text{-}axis}}$ *vs* position $\mathbf{P_{i\text{-}axis}}$, torque $\mathbf{T_{i\text{-}axis}}$ *vs* orientation $\mathbf{O_{i\text{-}axis}}$

3.2 Robot modeling

The classical dynamic model of a robot manipulator can be written in the Lagrangian form [6]:

$$\Gamma = \mathbf{M}(\mathbf{q})\ddot{\mathbf{q}} + \mathbf{C}(\mathbf{q},\dot{\mathbf{q}})\dot{\mathbf{q}} + \mathbf{G}(\mathbf{q}) \quad (1)$$

$\mathbf{q}$ is the vector of generalized coordinates. Γ is the vector of the torques of actuators. $\mathbf{M}(\mathbf{q})$ is the definite positive inertia matrix. $\mathbf{C}(\mathbf{q},\dot{\mathbf{q}})$ is the matrix of the Coriolis and centrifugal effects. $\mathbf{G}(\mathbf{q})$ is the vector of the gravity effects. This model is valid when the robot is considered without external force other than gravity. Including this model into the control scheme, the mechatronic system can be correctly driven by a PID controller.

However, the compacting roller is in contact with a stiff surface. So there is interaction between the robot and the workpiece due to the compacting strength. Moreover, the umbilical fibers guide disturbs the system. Consequently, we have to add external effort $\mathbf{J^T F_{ext}}$ where $\mathbf{J}$ is the Jacobian matrix of the effector expressed in the reference frame R_0 called world frame:

$$\Gamma + \mathbf{J^T F_{ext}} = \mathbf{M}(\mathbf{q})\ddot{\mathbf{q}} + \mathbf{C}(\mathbf{q},\dot{\mathbf{q}})\dot{\mathbf{q}} + \mathbf{G}(\mathbf{q}) \quad (2)$$

To change the dynamic model of the system, it would have access to the robot controller. To take into account the external forces, a sensor-based control has to be implemented.

4 Sensor-based control

4.1 Force sensor

The compacting strength $\mathbf{F_z}$ and the torque $\mathbf{T_x}$ have to be controlled. So, we use an ATI 6 DOF force/torque sensor. This type of sensor is already used and tested in the frame of chirurgical applications [7]. This sensor is attached on the wrist of the robot between the laying head and the arm manipulator (Fig.5). It can be integrated on the robot through the RSI module (Robot Sensor Interface). It measures forces and torques applied to x-axis, y-axis and z-axis. To have forces and torques at contact point, transporting force must be computed from sensor frame to contact point frame.

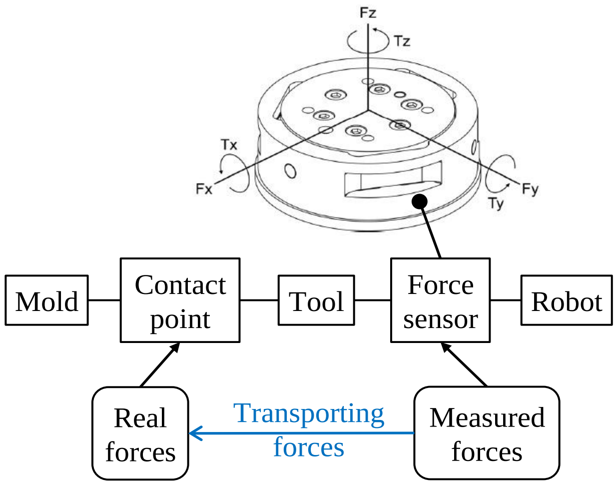

Fig.5. Force sensor

4.2 External hybrid control

Because we work in industrial context, the position control loop of the controller is inaccessible for warranty system issues. So we have to add an external loop to allow the control of forces [8]. Moreover, this command is already used in industrial applications like grinding and deburring [9]. This one converts the delta of force $\mathbf{\Delta F}$ in delta of position $\mathbf{\Delta X_f}$ for the inner loop through the force control law (Fig.6). The dual command (position/force) can be managed in the Cartesian space. In this way, the theoretical tool-path can be followed while applying a controlled compacting strength $\mathbf{F_z}$ [10] and a zero torque $\mathbf{T_x}$. The diagonal selection matrix $\mathbf{S}$ allows choosing the directions controlled in force ($s_i = 0$) and the directions controlled in position ($s_i = 1$) as $\mathbf{S} = \mathbf{Diag}(s_1, s_2, \ldots, s_6)$.

In Fig.6, we can see the mechanism of the external hybrid position-force control. First, the force-torque desired $\mathbf{F_{des}}$ is compared to the force-torque measured $\mathbf{F_{meas}}$. This delta $\Delta\mathbf{F}$ must be converted in delta of position $\Delta\mathbf{X_F}$ through the force control law. Simultaneously, the position-orientation desired $\mathbf{X_{des}}$ is compared to the position-orientation measured $\mathbf{X}$. This delta $\Delta\mathbf{X}$ is converted in $\Delta\mathbf{X_P}$ through the position control law. Then, the delta of position $\Delta\mathbf{X_{FP}}$ is composed of directions controlled in force, and other directions controlled in position thanks to the selection matrix $\mathbf{S}$, and is sent to the RSI module. This one is added to the current position and is sent to the inner position control loop. A PID correction is implemented on the force control law concerning the compacting strength $\mathbf{F_z}$ and the torque $\mathbf{T_x}$. In this way, delta on z-direction and delta around x-orientation are computed according to the force and torque errors.

5 Experimental

5.1 Test environment

5.1.1 Hardware architecture

The robotic cell of ESTIA (Fig.7) is used for preliminary testing. It consists of a KUKA KR6 robot with RSI module to allow sensors integration. This manipulator has the same kinematics as the robot KUKA KR240, only inertial and dimensional parameters change. A compaction roller and its support are added on the system. A plate is put on the table and the robot makes the movement on it.

5.1.2 RSI module

The RSI module is an intermediary system between the robot controller and the force sensor. In our RSI configuration, we choose to work with a delta of position-orientation of the tool as input data in the tool frame as application frame. Then, it adds this delta to the current position-orientation of the tool in the reference frame. Finally, it sends the Cartesian position of the tool in the reference frame to the robot controller.

With the robot controller KRC2, the RSI module must receive data in a period of 12 ms, otherwise data is lost. This data is transmitted in XML format.

Here is an example of communication data frame:

<Sen Type="PCext">
<DeltaPos X="0" Y="0" Z="0" A="0" B="0" C="0" />
<IPOC>123645634563</IPOC>
</Sen>

With:

- PCext: identity of the sending machine frame
- DeltaPos: delta of position/orientation to apply in comparison to the current position/orientation
- IPOC: ID number of the frame

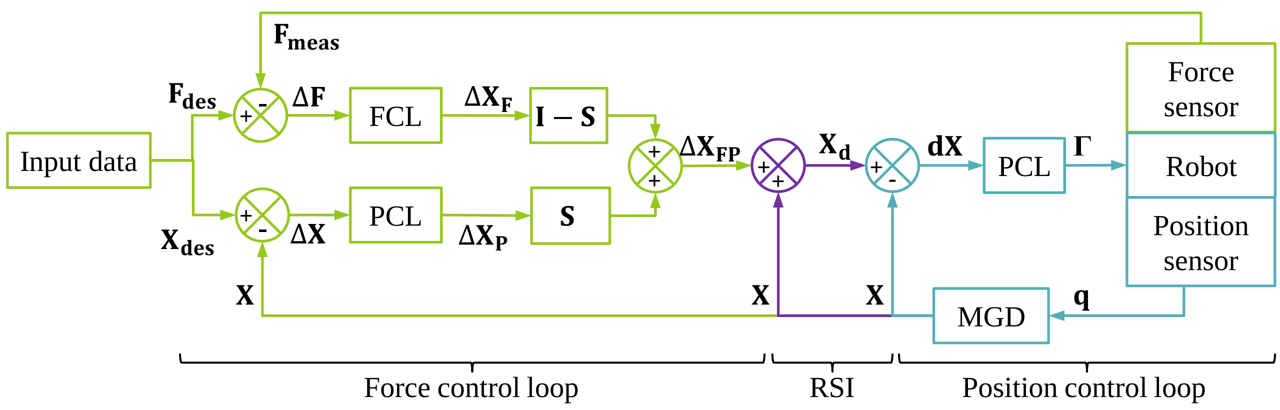

FCL: Force Control Law; PCL: Position Control Law; RSI: Robot Sensor Interface;
$\mathbf{F_{des}}$: Forces-torques desired; $\mathbf{F_{meas}}$: Forces-torques measured; $\Delta\mathbf{F} = \mathbf{F_{des}} - \mathbf{F_{meas}}$; $\Delta\mathbf{X_F}$: Delta of position-orientation to correct force and torque; $\mathbf{I} - \mathbf{S}$: allows to control $\mathbf{F_z}$ and $\mathbf{T_x}$; $\mathbf{X_{des}}$: Position-orientation desired; $\mathbf{X}$: Current position-orientation in the reference frame; $\Delta\mathbf{X} = \mathbf{X_{des}} - \mathbf{X}$; $\Delta\mathbf{X_P}$: Delta of position-orientation to correct position and orientation; $\mathbf{S}$: allows to control specific directions in position-orientation; $\Delta\mathbf{X_{FP}}$: Delta of position-orientation to do; $\mathbf{X_d} = \mathbf{X} + \Delta\mathbf{X}$: Position-orientation desired in Cartesian space for the control position loop; $\mathbf{dX} = \mathbf{X_d} - \mathbf{X}$; $\mathbf{\Gamma}$: Vector of the torques of actuators; $\mathbf{q}$: Vector of joints.

Fig.6. External hybrid position/force control

5.1.3 Software architecture

A client-server type communication is developed between elements. In this way, the client “robot” can communicate with the client “sensor” thanks to the application server via a TCP/IP communication. In fact, current position-orientation of the tool in the reference frame is sent to the RSI module by the robot. This one is transmitted to the server and then to the client “sensor”. At the same time, this client receives force-torque through the force sensor. Consequently, the desired correction can be computed and sent to the server, which transmits it to the RSI module and then executed on the robot.

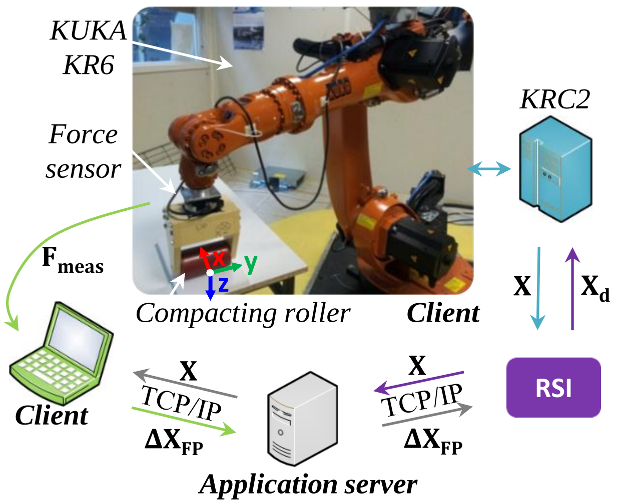

Fig.7. Test environment

5.1.4 Implementation

The development of server and clients was made in C# language using Visual Studio environment. Server has no particular interface. However, Fig.8 shows the client interface which is composed of four parts.

Force: (surrounded in green). The area A allows sensor calibration and doing a bias of data to remove the gravity effect. The area E shows force and torque measurements. The area G allows choosing which direction is force controlled. In accordance with the selection matrix (Fig.6), the direction controlled in force cannot be controlled in position.

RSI module: (surrounded in purple). The area B allows connecting to the server in order to communicate with the RSI module. The area H manages the trajectory generation by linear movement for RSI module.

Robot: (surrounded in blue). The area D shows the joint values of robot and the area F shows the Cartesian values of the tool in the reference frame. These values are updated every 12 ms.

Log: (surrounded in black). Every 12 ms, data are recorded in text file that can be opened in Matlab for analysis and display. Data is composed of position-orientation of the tool in reference frame [x,y,z,A,B,C] and wrench measures [Fx,Fy,Fz,Tx,Ty,Tz].

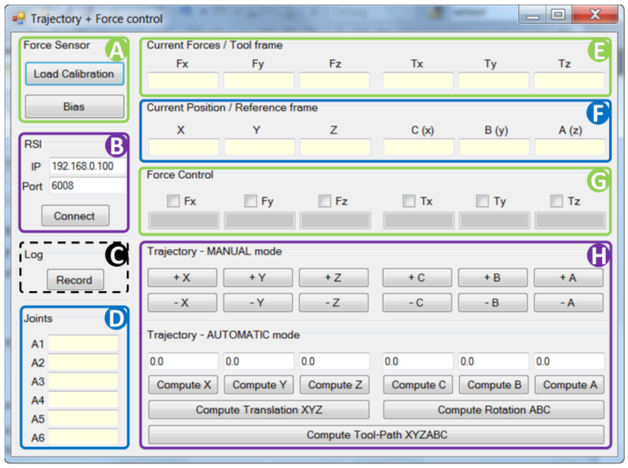

Fig.8. C# interface of client « force sensor »

5.2 Test procedures

We have to establish relation between tool position on mold and the resulting forces. To do that, tests are made with position control mode and hybrid position/force control mode in order to see the difference between these two control modes on resulting forces (Fig.9).

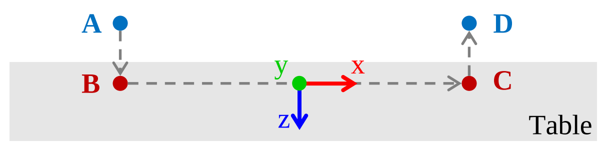

Fig.9. Robot path

5.2.1 Position control mode

In this mode, to obtain the compacting strength, the contact point is modified and it is defined under the mold surface. The tool goes down on the mold until a -8 N contact force is reached (A→B). Then, the robot is controlled in position to make a movement of *dx* following x-axis (B→C). Finally, the robot is lifted through manual control (C→D). Observation of forces and torques in relation to positions and orientations of the tool allows establishing relation between tool positions on mold and resulting forces.

5.2.2 Hybrid position/force control mode

In this mode, the compacting strength is controlled in closed loop. The procedure for the movements (A→B) and (C→D) does not change. However, for the movement (B→C), the robot is controlled in position following x-axis to make the displacement of *dx* millimeters and it is controlled in force following z-axis to have a compacting strength $\mathbf{F_z}$ of -8 N throughout the advance. Here, the compacting strength should be close to the setpoint even if the mold surface is slightly different.

5.2.3 Study cases

Experimentations have been made on four study cases (Fig.10):

Case 1: The mold is placed on the table which is considered planed.

Case 2: A defect is placed under the mold to disturb the compacting strength $\mathbf{F_z}$.

Case 3: A block is placed under the mold in order to have an inclination with an angle about 3°. This case illustrates the case of a ramp in the fiber placement.

Case 4: A defect is placed under the mold to disturb the force distribution and generates a torque $\mathbf{T_x}$.

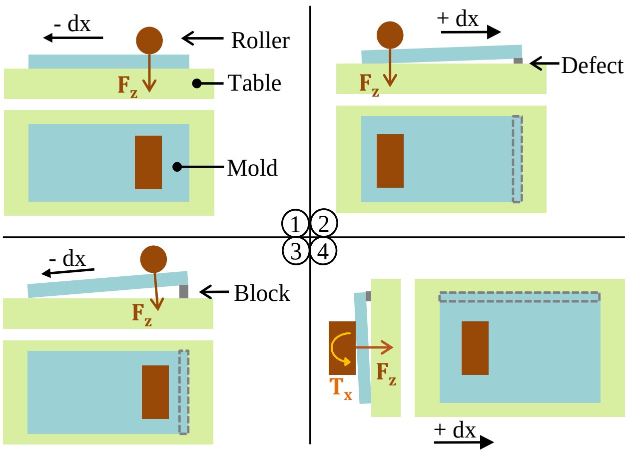

Fig.10. Study cases

5.3 Results

Analysis of tests results allows a qualitative study of the added force control in the compacting direction in relation to the disturbances. The idea is to study the relation between the force control and the accurate fiber placement. The study is made between points B and C (Fig.9).

5.3.1 Case 1

First, the system is controlled in position as the actual implementation (Fig.11). When the tool moves along x-axis ($^{\mathbf{world}}\mathbf{x_{tool}}$), the tool position along z-axis($^{\mathbf{world}}\mathbf{z_{tool}}$) varies very slightly and the compacting strength increases very much. In fact, it is considered as flat but the compacting strength ($^{\mathbf{tool}}\mathbf{F_z}$) is equal to -8 N at the beginning and then, but grows up to -40 N. Moreover, force along y-axis appears.The measurement is negative because force sensor measures interaction of mold on the tool and not interaction of the tool on mold.

Secondly, the system is controlled with hybrid position/force control mode (Fig.11). Here, the tool position is corrected along z-axis ($^{\mathbf{world}}\mathbf{z_{tool}}$) in order to maintain the compacting strength desired. The measured force along z-axis ($^{\mathbf{tool}}\mathbf{F_z}$) varies quickly according to the tool position. In fact, the tool needs to move down around 0.8 mm along z-axis to keep the compacting strength and there are oscilllations around the setpoint of -8 N during the displacement. We can observe that the force along y-axis has decreased.

5.3.2 Case 2

First, the system is controlled in position (Fig.12). When the tool moves along x-axis ($^{\mathbf{world}}\mathbf{x_{tool}}$), the tool position along z-axis ($^{\mathbf{world}}\mathbf{z_{tool}}$) varies very slightly and the compacting strength varies very much according to mold deformation and its stifness. It is considered as flat but the compacting strength ($^{\mathbf{tool}}\mathbf{F_z}$) is equal to -8 N at the beginning then it is equal to -5 N and finally to -16 N.

Secondly, the system is controlled with hybrid position/force control mode (Fig.12). Here, the tool position is corrected along z-axis ($^{\mathbf{world}}\mathbf{z_{tool}}$) in order to maintain the compacting strength desired. We can see the deformation mold with the displacement along z-axis.

5.3.3 Case 3

First, the system is controlled in position (Fig.13). When the tool moves along x-axis ($^{\mathbf{world}}\mathbf{x_{tool}}$), the compacting strength varies very much according to the deformation mold and its stiffness. The compacting strength ($^{\mathbf{world}}\mathbf{F_z}$) is equal to -8 N at the beginning and finally to -22 N with intermediate changes.

Secondly, the system is controlled with hybrid position/force control mode (Fig.13). Here, the tool position is corrected along z-axis ($^{\mathbf{world}}\mathbf{z_{tool}}$) in order to maintain the compacting strength desired.

5.3.4 Case 4

First, the system is controlled in force only for the compacting strength $^{tool}\mathbf{F_z}$ (Fig.14). When the tool moves along x-axis ($^{world}\mathbf{x_{tool}}$), the compacting strength varies very slightly around the setpoint of -8 N. However, a torque appears around x-axis because of the defect.

Secondly, the system is controlled in force for the compacting strength $^{tool}\mathbf{F_z}$ and the torque $^{tool}\mathbf{T_x}$ (Fig.14). Here, the compacting strength is disturbed by the correction of the torque which varies a little about 0 Nm.

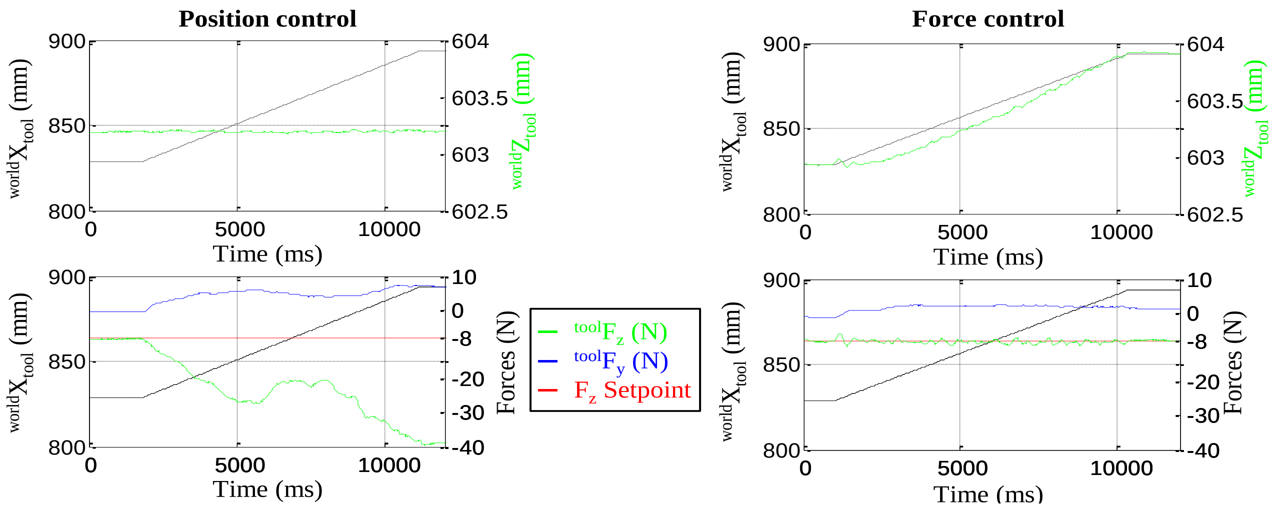

Fig.11. Case 1

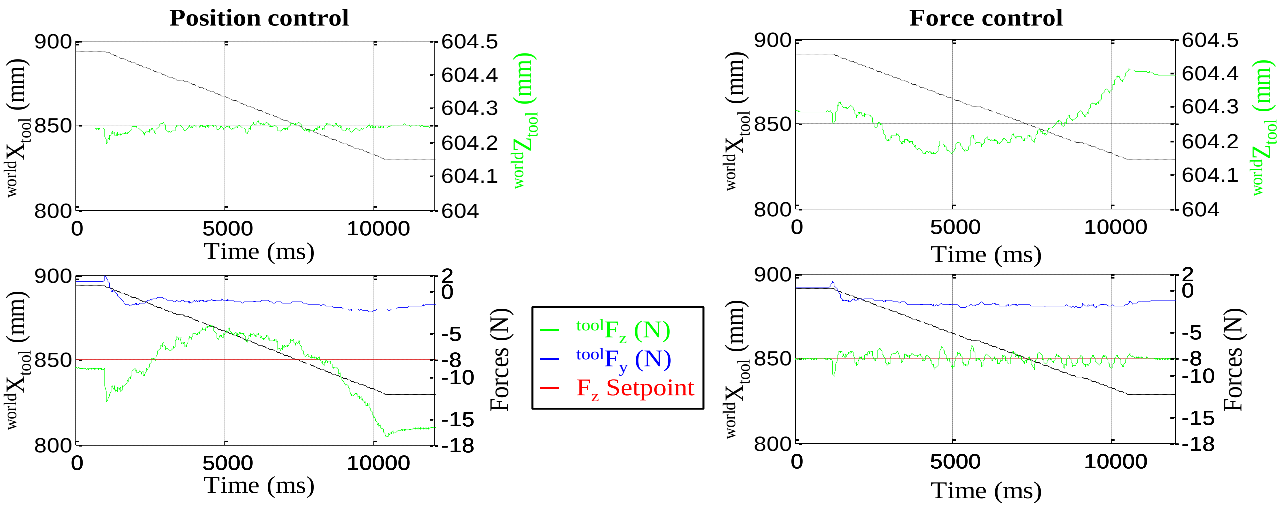

Fig.12. Case 2

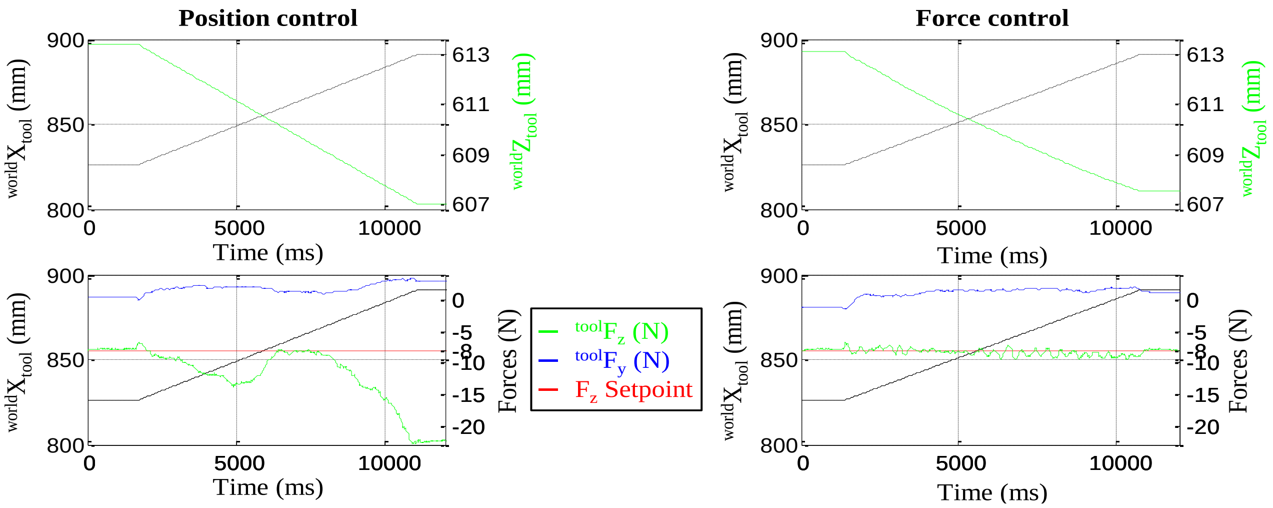

Fig.13. Case 3

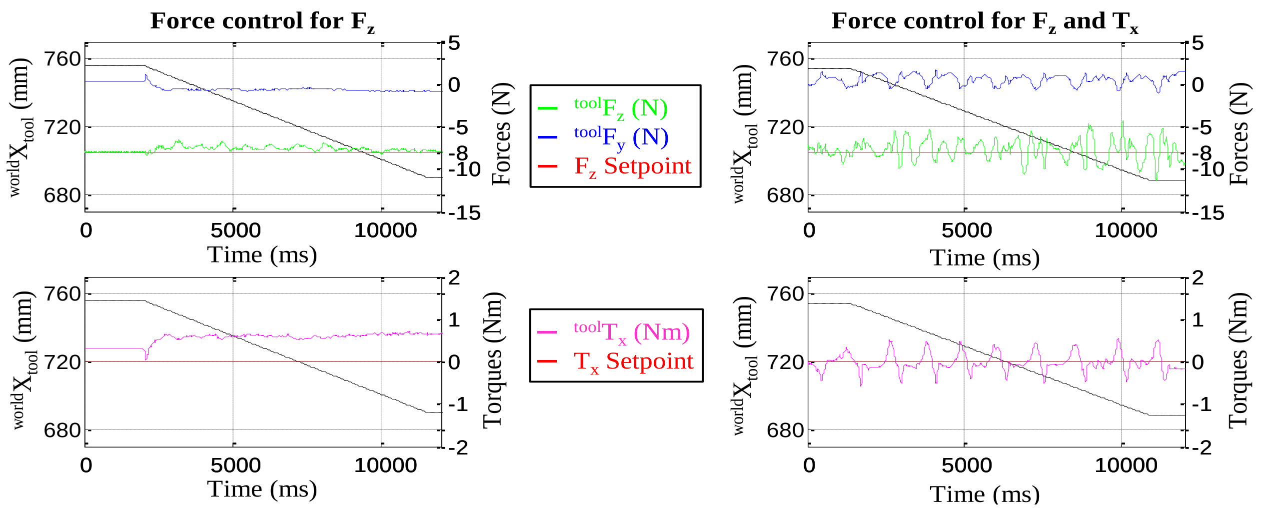

Fig.14. Case 4

6 Conclusion & Future works

To control the compacting strength in the industrial robotic context, we have implemented an external hybrid command. This helped us in understanding the origin of inaccuracies.

The first results show that if the mold placement is not corresponding to the theoretical position used in CATfiber for trajectory definition, the position control mode is not sufficient to maintain required compacting forces. However, the hybrid position/force control has a positive impact on the system to improve its accuracy. In fact, the disturbant force along y-axis has been decreased. Quantitative measurements must be performed to validate this decrease.

Today, PID settings are very specific to a given situation: type of compacting roller, stiffness of the mold and compacting strength desired. Consequently, the impact of the roller stiffness on the control of the compacting strength should be studied to optimize the PID settings.

We plan to identify the model to determine its parameter and to complexify the force control to make it more efficient with better choice of controller gains.

To characterize the respect of the fiber placement location we need a tool which shows us the improvement of the laying quality. To do that, the use of exteroceptive sensors like laser traker and BOM camera is considered.

Acknowledgement

This research work was done in the frame of the IMPALA project, a French funded project from FUI-011 program, under the convention n°F 11 08 008 B. The project consortium is composed by Coriolis Composites, Dassault Aviation, Daher-Socata, Composites Aquitaine (an EADS Sogerma company), CompositAdour, Ecole Centrale de Nantes and ESTIA.

References

[1] «Les matériaux composites, dynamisme et innovation», les 4 pages des statistiques industrielles, n°158, Février 2002. http://www.insee.fr/sessi/4pages/pdf/4p158.pdf

[2] Overview of the worldwide composites industry: 2010-2015, strategic study, JEC Composites.

[3] http://www.eucia.org/uploads/5bb0a32f9232921767ffdace468e27a5.pdf. Composites Market Report 2011: Market developments, trends, challenges and opportunities. The European GRP market – Dr. Elmar Witten (AVK) , The global CRP market – Bernhard Jahn (CCeV)

[4] «La dynamique des nouveaux procédés», l'usine nouvelle n°3093, mars 2008. http://www.usinenouvelle.com/article/la-dynamique-des-nouveaux-procedes.N60471

[5] N.J.Johnston, H.L.Belvin, R.J.Cano, J.M Marchello, and A.B.Hulcher. «A prototype research laboratory for automated fabrication of high performance composites». *ICCM 12*. 1999, Paris, France

[6] Dung Le Tien, Kang Hee-Jun, and Ro Young-Shick. «Robot manipulator modeling in Matlab-SimMechanics with PD control and online gravity compensation». *International Forum on Strategic Technology* 2010, pages 446–449. IEEE, October 2010.

[7] Nabil Zemiti. «Commande en Effort des Systèmes Robotiques pour la Chirurgie Mini-Invasive». PhD thesis, LRP, Paris 6 University, Paris, France 2006

[8] J. De Schutter and H. Van Brussel. Compliant Robot Motion II. A Control Approach Based on External Control Loops. *The International Journal of Robotics Research*, 7(4): 18–33, August 1988.

[9] A. Robertsson, T. Olsson, R. Johansson, A. Blomdell, K. Nilsson, M. Haage, B. Lauwers, H. Baerdemaeker, T. Brogardh, and H. Brantmark. «Implementation of Industrial Robot Force Control Case Study: High Power Stub Grinding and Deburring». In 2006 *IEEE/RSJ International Conference on Intelligent Robots and Systems*, pages 2743–2748. IEEE, October 2006.

[10] E. Dégoulange, P. Dauchez, and F. Pierrot. «Determination of a force control law for an industrial robot in contact with a rigid environment». *IEEE Int. Conference on SMC*, Le Touquet, France, Vol. 2, pp. 270-275, 1993.